6624 *Biochemistry* **2009,** *48,* 6624–6632
DOI: 10.1021/bi900755n

BIOCHEMISTRY
including biophysical chemistry & molecular biology
Article

In Vitro Enzymatic Characterization of Near Full Length EGFR in Activated and Inhibited States[†]

Chen Qiu,[‡,⊥] Mary K. Tarrant,[§,⊥] Tatiana Boronina,[∥] Patti A. Longo,[‡] Jennifer M. Kavran,[‡] Robert N. Cole,[∥] Philip A. Cole,*[,§] and Daniel J. Leahy*[,‡]

[‡]*Department of Biophysics and Biophysical Chemistry,* [§]*Department of Pharmacology and Molecular Sciences,* [∥]*Mass Spectrometry/Proteomics Facility at Johns Hopkins University School of Medicine, and Johns Hopkins University School of Medicine, Baltimore, Maryland 21204.* [⊥]*These authors contributed equally to this work*

Received May 1, 2009; Revised Manuscript Received June 10, 2009

ABSTRACT: The epidermal growth factor receptor (EGFR) is a single-pass transmembrane protein with an extracellular ligand-binding region and a cytoplasmic tyrosine kinase. Ligand binding activates the tyrosine kinase, which in turn initiates signaling cascades that influence cell proliferation and differentiation. EGFR activity is essential for normal development of many multicellular organisms, and inappropriate activation of EGFR is associated with multiple human cancers. Several drugs targeting EGFR activity are approved cancer therapies, and new EGFR-targeted therapies are being actively pursued. Much of what is known about EGFR structure and function is derived from studies of soluble receptor fragments. We report here an approach to producing an active, membrane-spanning form of EGFR of suitable purity, homogeneity, and quantity for structural and functional studies. We show that EGFR is capable of direct autophosphorylation of tyrosine 845, which is located on its kinase activation loop, and that the kinase activity of EGFR is ~500-fold higher in the presence of EGF vs the inhibitory anti-EGFR antibody cetuximab. The potencies of the small molecule EGFR kinase inhibitors erlotinib and lapatinib for various forms of EGFR were measured, and the therapeutic and mechanistic implications of these results considered.

The epidermal growth factor receptor (EGFR[1]) was the first cell-surface receptor shown to have intrinsic tyrosine kinase activity and is thus the archetype of a class of receptors, now numbering over 50 in humans, that includes receptors for insulin, VEGF, NGF, ephrins, and FGF (*1*, *2*). These receptors, known as receptor tyrosine kinases (RTKs), consist of an extracellular ligand binding region, a single membrane-spanning region, and a cytoplasmic tyrosine kinase. EGFR and several other RTKs also include a C-terminal tail that harbors several autophosphorylation sites (*3*). RTKs transmit information across the cell membrane by adopting specific dimeric conformations in response to ligand binding, which in turn leads to activation of the intracellular kinase activity, autophosphorylation, and initiation of intracellular signaling cascades (*4*, *5*).

Four EGFR homologues, EGFR (HER1/ErbB1), HER2 (ErbB2/Neu), HER3 (ErbB3), and HER4 (ErbB4), exist in humans and are collectively known as the EGFR, HER, or ErbB family of receptors (*6*). Each EGFR homologue mediates key cell proliferation and differentiation events, and loss of any family member results in severe developmental defects or embryonic lethality (*7*). In adults, inappropriate expression or activation of EGFR homologues has been associated with multiple human cancers (*8*), and drugs targeting ErbB activity have been approved for treatment of breast, colon, lung, and head-and-neck cancers. These drugs are of two types: monoclonal antibodies targeting ErbB extracellular regions, which include the anti-EGFR antibodies cetuximab (Erbitux) and panitumumab (Vectibix) and the anti-HER2 antibody trastuzumab (Herceptin), and small molecule kinase inhibitors, which include erlotinib (Tarceva), gefitinib (Iressa), and lapatinib (Tykerb) (*9*).

The extracellular regions of ErbBs comprise four independent domains identifiable in both primary and tertiary structures, and structural studies of active ErbB fragments have led to the characterization of receptor conformations that appear correlated with specific functional states (*10*, *11*). In the absence of ligand, the extracellular regions of EGFR, HER3, and HER4

[†]This work was supported by NIH Grants CA090466 (to D.J.L.) and CA74305 (to P.A.C.).

*Corresponding author. 725 N. Wolfe St., Baltimore, MD 21204. Tel: 410-614-2534. Fax: 410-955-0637. E-mail: dleahy@jhmi.edu (D.J.L.); pcole@jhmi.edu (P.A.C.).

[1]Abbreviations: CHO, Chinese hamster ovary; DTT, dithiothreitol; EDTA, ethylene diamine tetraacetic acid; EGF, epidermal growth factor; EGFR, EGF receptor; EGTA, ethylene glycol tetraacetic acid; FGF, fibroblast growth factor; FPLC, fast protein liquid chromatography; HEK, human embryonic kidney; HEPES, 4-(2-hydroxyethyl)-1-piperazineethanesulfonic acid; HPLC, high pressure liquid chromatography; iTRAQ, isobaric tag for relative and absolute quantitation; LCMS/MS, liquid chromatography tandem mass spectrometry; NGF, nerve growth factor; Ni-NTA, nickel-nitrilotriacetic acid; PBS phosphate-buffered saline; PEI, polyethylenimine; RTK, receptor tyrosine kinase; SCX, strong cation exchange; MS/MS, tandem mass spectrometry; SDS−PAGE, sodium dodecyl sulfate−polyacrylamide gel electrophoresis; TEAB, triethylammonium bicarbonate; tEGFR, truncated EGFR; TEV, tobacco etch virus; TFA, trifluoroacetic acid; VEGF, vascular endothelial growth factor.

 Published on Web 06/11/2009

adopt a "closed" structure in which an extended β-hairpin from domain 2 is buried in a contact near the juxtamembrane region of domain 4 (*10*, *12*−*14*). This contact constrains the extracellular region into an arrangement in which ligand-binding surfaces on domains 1 and 3 are too far apart to bind the ligand simultaneously. When the ligand is bound, domains 1 and 3 become juxtaposed, the contact between domains 2 and 4 is broken, and the hairpin loop on domain 2 mediates receptor dimerization (*10*, *15*, *16*). Activation of the intracellular kinase activity relies on the formation of a specific "asymmetric" dimer of the kinase domains (*11*), and formation of the extracellular dimer must promote the formation of this asymmetric dimer. How the extracellular dimer promotes intracellular dimer formation and kinase activation is not apparent from studies with receptor fragments, however, and many outstanding questions concerning interactions and communication between different regions of the receptor remain.

Quantitative enzymological studies of ErbBs have also been primarily limited to soluble, active fragments of receptor intracellular domains or incompletely characterized whole receptor (*11*, *17*−*20*). Although much has been learned from these studies, a complete picture of EGFR kinase activity is necessarily lacking. To enable structural and functional studies of an intact form of EGFR, we have developed a strategy to produce a membrane-spanning form of EGFR that is of sufficient purity, homogeneity, and quantity for structural, biophysical, and enzymological studies. Our approach shares many features with one recently reported by Springer and colleagues (*21*). We have used our purified EGFR to demonstrate direct autophosphorylation of Y845 and make quantitative enzymological measurements of active and inhibited forms of EGFR.

MATERIALS AND METHODS

Reagents. Lapatinib was synthesized as previously described (*20*, *22*). Pharmaceutical erlotinib was obtained from C. Rudin of Johns Hopkins and purified in the Johns Hopkins Synthetic Core facility using silica gel chromatography. Pharmaceutical cetuximab was obtained from C. Hann and C. Rudin (Erbitux lot# 18148, manufacture date 1/27/03), and the Fab portion of the cetuximab obtained by digestion of the antibody with papain followed by anion exchange chromatography using FPLC. PP2 was obtained from Calbiochem. Acetonitrile (MS grade, J.T. Baker), formic acid (98−100% "suprapure", EMD), phosphoric acid (Puriss grade, Fluka), trifluoroacetic acid (neat, Supelco), Trypsin (sequencing grade, Promega). All aqueous solutions were prepared using Milli-Q water (Millipore). The anti-pY845 antibody (Life Sciences) was a gift from Mark Lemmon of the University of Pennsylvania.

Purification of EGF. The gene encoding human EGF was inserted into the pT7HT vector (*27*), transfected into *E. coli*, and expression induced by addition of isopropyl-β-D-thiogalactopyranoside followed by growth for at least 3 h at 37 °C. Cells were lysed in 6 M guanidine hydrochloride, centrifuged, and the supernatant loaded onto a Ni-NTA column. After washing, the column was eluted with 200 mM imidazole, and 5 mM dithiothreitol was added to pooled EGF-containing elution fractions. EGF was refolded by rapid dilution into 0.1 M Tris, pH 8.0, and 50 mM NaCl, dialyzed overnight, and rerun on a Ni-NTA column. After elution from the Ni-NTA column, TEV protease was used to remove the histidine tag. EGF was then concentrated and chromatographed on a Superdex 75 size exclusion column (GE Healthcare). Peak fractions were pooled and concentrated.

Transfection of HEK293 GnTi$^-$ *Cells*. A cDNA encoding human EGFR was mutagenized using the megaprimer method to introduce a hexahistidine tag encoding region and a stop codon immediately following the position encoding Gly 998 (numbering from the mature N-terminus) (*23*). The resulting cDNA, which encodes a truncated form of EGFR (tEGFR), was subcloned into the pLEXm expression vector using the NotI and XhoI cloning sites (*24*).

Four hundred milliliter suspension cultures of HEK293 GnTi$^-$ cells were seeded with 0.2×10^6 cells/mL and allowed to grow to $2-2.5 \times 10^6$ cells/mL (3−4 days) in Freestyle 293 medium (Invitrogen 12338) supplemented with 1% FBS (Invitrogen 10437) and 2 mM glutamine (Invitrogen 25030) (*25*). No antibiotics were used. Cells were incubated at 37 °C, 8% CO_2 and shaken at 130 rpm in square bottles (Fisher 033112E) (*26*). Cells were harvested at 4 °C by centrifugation for 5 min at 1000 rpm and resuspended in 400 mL of fresh medium for transfection. For transfection, a 1 mg/mL stock of linear PEI MAX (Polyscience 24765) that had been neutralized with NaOH and sterile filtered was combined in a 3:1 weight ratio with sterile filtered expression plasmid DNA. Typically, 1.2 mL of PEI stock solution was added to 8.8 mL of Hybridoma medium (Invitrogen 12045), and 400 μg of expression plasmid DNA added to a separate tube of 10 mL of Hybridoma medium. The PEI and DNA containing media were combined (20 mL total), gently mixed, incubated for 20 min at room temperature, and added to the prepared cells. After 24 h, the cells were diluted 1:1 with fresh medium, split into two 400 mL bottles, and incubated at 37 °C with shaking for another 72 h.

Purification of tEGFR. Transfected HEK293 GnTi$^-$ cells were harvested by centrifugation at 3000 rpm for 10 min, washed with phosphate-buffered saline (PBS), and either used directly or frozen at −20 °C. Cells were lysed by the addition of an equal volume of homogenization buffer (40 mM HEPES at pH 7.4, 10 mM EGTA, 2% Triton X-100, 20% glycerol, and a protease inhibitor cocktail (Roche)). Cells were then sonicated in three 20-s bursts and centrifuged at 14,000 rpm. The supernatant was filtered, beads covalently modified with the anti-EGFR monoclonal antibody 528 (*28*) were added, and the slurry was incubated overnight at 4 °C with gentle shaking. The beads were then transferred to a column and washed in succession with (i) 25 mL of receptor buffer (20 mM HEPES at pH 7.4, 150 mM NaCl, 1 mM EDTA, 0.5 mM dithiothreitol, 10% glycerol, and 0.03% Dodecylmaltoside), (ii) 25 mL of receptor buffer/1 M NaCl, (iii) 25 mL of receptor buffer, (iv) 25 mL of receptor buffer/1 M NaCl, (v) 25 mL of receptor buffer, (vi) 25 mL of receptor buffer/1 M Urea, and (vii) 50 mL of receptor buffer.

The column was then eluted with 5 successive additions of an equal volume of 25 μg/mL EGF or 0.1 mg/mL cetuximab Fab in receptor buffer that were incubated on the column for 30 min at room temperature. Each elution fraction was collected and pooled. A 1:1000 dilution by volume of 1 mg/mL stock solutions of endoglycosidases H and F was added to the pooled fractions (10 μL of each stock solution per 10 mL protein solution) and incubated at 4 °C for 1 h. The protein solution was then concentrated to no more than 500 μL total volume using a 100 kD molecular weight cut off Amicon Ultra-4 (Millipore) and loaded onto a Superose 6 size exclusion column and chromatographed in 20 mM HEPES at pH 7.4, 150 mM NaCl, 0.5 mM DTT, 5% glycerol, and 0.03% dodecylmaltoside. Elution fractions containing tEGFR were identified by Western blot, pooled, and concentrated. Purified tEGFR was quantitated using UV absorbance and comparison of bands of tEGFR and bovine

serum albumin standards on Coomassie Blue-stained SDS−PAGE gels.

Western Blots. Three micromolar tEGFR/EGF complex was incubated in reaction buffer (20 mM Hepes, pH 7.4, 1 mM $MnCl_2$, 5 mM $MgCl_2$, 1 mM ATP, and 1 mM Na_3VO_4) for 10 min at room temperature (~22 °C). The reaction was stopped by the addition of SDS gel loading buffer and the proteins resolved on SDS−PAGE followed by Western blotting using either the antiphosphotyrosine antibody 4G10 or a specific anti pY845 antibody (Life Sciences).

Kinase Assays. To determine the kinetic parameters for the EGF/tEGFR and cetuximab Fab/tEGFR complexes, radiometric kinase assays were carried out in 50 mM HEPES (pH 7.5), 37.5 mM NaCl, 1 mM DTT, 5% glycerol, 125 μg/mL BSA with either 2 mM $MnCl_2$ or 10 mM $MgCl_2$, and Biotin-RA-HEEIYHFFFAKKK-COOH as the peptide substrate in a 25 μL reaction volume. The peptide substrate was prepared using standard Fmoc solid-phase peptide synthesis followed by coupling of biotin to the N-terminus using the biotin *p*-nitrophenyl ester (NovaBiochem) and purification by reverse phase HPLC. Reactions were initiated by the addition of kinase, carried out at 30 °C, and stopped by the addition of 10 μL of 100 mM EDTA. To each sample, 10 μL of 10 mg/mL avidin (Thermo Scientific) was added, and all samples were transferred to centrifugal filtration units with 30,000 nominal molecular weight limit membranes (Millipore) and washed three times with 100 mL of wash solution (0.5 M phosphate and 0.5 NaCl, pH 8.5). The limiting substrate turnover was less than 10% for all rate measurements. Duplicate measurements were generally within 20%.

The linear range for activity vs time was established using multiple time points, 80 μM peptide, either 2 mM $MnCl_2$ or 10 mM $MgCl_2$, 100 μM ATP, and 25 nM enzyme (except for the cetuximab Fab/tEGFR complex with 10 mM $MgCl_2$, which used 50 nM enzyme). The linear range for activity vs enzyme concentration was established using various enzyme concentrations, 80 μM peptide, either 2 mM $MnCl_2$ or 10 mM $MgCl_2$, and 100 μM ATP.

The K_m^{app} for peptide substrate was determined with varying peptide concentrations and fixed ATP concentration (100 μM). Assays for EGF/tEGFR used 25 nM enzyme and the following peptide concentrations: 1.88, 3.75, 7.5, 15, 30, 60, and 120 μM. Assays for cetuximab Fab/tEGFR used 125 nM enzyme and the following peptide concentrations: 6.25, 12.5, 25, 50, 100, 200, 400, and 800 μM. The K_m^{app} for ATP was determined by using varying ATP concentrations and fixed peptide substrate concentration. Assays for EGF/tEGFR used 25 nM enzyme and the following ATP concentrations in the presence of 2 mM $MnCl_2$: 0.78, 1.56, 3.13. 6.25, 12.5, 25, 50, and 100 μM. Assays for EGF/tEGFR used 25 nM enzyme and the following ATP concentrations in the presence of 10 mM $MgCl_2$: 3.75, 7.5, 15, 30, 40, 60, 90, 120 μM. Assays for cetuximab Fab/tEGFR used 125 nM enzyme and the following ATP concentrations: 1.56, 3.13, 6.25, 12.5, 25, 50, 100 μM. Apparent K_m and k_{cat} values were obtained from nonlinear curve fits to the Michaelis−Menten equation.

For the IC_{50} determination for lapatinib, various concentrations of lapatinib (40, 10, 2.5, 0.625, 0.313, 0.159, and 0.078 μM) were preincubated with enzyme on ice for 10 min and the reactions run with 10 μM ATP, 30 μM peptide, 2 mM $MnCl_2$, 25 nM enzyme, and 0.15% DMSO for 6 min with EGF/tEGFR and for 40 min with cetuximab Fab/tEGFR. For the IC_{50} determination for erlotinib, the inhibitor erlotinib (160, 40, 10, 2.5, 0.625, 0.313, 0.159, and 0.078 μM) was preincubated with enzyme at 30 °C for 10 min, and the reactions were run with 10 μM ATP, 30 μM peptide, 2 mM $MnCl_2$, 25 nM enzyme, and 0.15% DMSO for 5 min with EGF/tEGFR and for 40 min with cetuximab Fab/tEGFR. IC_{50} values were obtained from fitting the isotherm from the dose−response plot.

Mass Spectrometric Analysis. *In-Gel Digestion*. The kinase reaction was carried out by incubating a 3 μM tEGFR/EGF complex in 15 μL of reaction buffer (20 mM Hepes, pH 7.4, 1 mM $MnCl_2$, 5 mM $MgCl_2$, 1 mM ATP, and 1 mM Na_3VO_4) for 30 min at 30 °C. The reaction was stopped by the addition of SDS gel loading buffer, and the proteins were resolved on SDS−PAGE. For the inhibitor experiment, 3 μM EGFR/EGF complex was preincubated with 200 μM erlotinib or PP2 for 30 min on ice before the addition of ATP-containing reaction buffer. The SDS−PAGE bands corresponding to EGFR at ~120 kDa tEGFR were excised, destained, and buffer exchanged by alternating acetonitrile and 50 mM TEAB (triethylammonium bicarbonate) washes. Protein bands were then digested with 10 ng/μL sequencing grade trypsin (Promega) in 35 μL of 50 mM TEAB for 16 h at 37 °C. Peptides were extracted with 55% acetonitrile containing 0.5%TFA (trifluoroacetic acid) and dried.

iTRAQ Labeling. Extracted peptides were resuspended in 10 μL of 0.5 M TEAB. Isopropanol (50 μL) was added to vials containing 113, 115, 117, or 121 iTRAQ-8plex reagent. Each sample was labeled for 2 h at room temperature by adding 25 μL of one iTRAQ reagent, maintaining the pH between 7.5 and 8.0 with 0.5 M TEAB. All four iTRAQ labeled samples were combined and dried. Approximately 8 μg of total labeled peptide (based on total protein loaded on the gel) was resuspended in 10 μL of 0.2%TFA, desalted using a C18 ziptip (Varian), eluted with 70% acetonitrile in 0.1%TFA, and dried.

Strong Cation Exchange (SCX) Chromatography. Desalted peptides were resuspended in 200 μL of SCX buffer A (10 mM potassium phosphate buffer, pH 2.85, and 25% acetonitrile). The sample was adjusted to pH 2.5−2.8 with phosphoric acid and loaded onto a PolySulfethyl A column (100 × 0.3 mm, 300 Å, 5 μm, PolyLC, Columbia, MD) at 5 μL/min for 40 min using an Agilent 1200 series capillary HPLC system. Peptides were fractionated using 0−100% SCX buffer B (350 mM KCl in 10 mM potassium phosphate buffer, pH 2.85, and 25% acetonitrile) linear gradient over 60 min at 5 μL/min. Fractions were collected manually (7 fractions, 40−100 μL fraction), dried, and stored at −80 °C until LCMS/MS analysis.

Mass Spectrometry. Each SCX fraction was redissolved in 40 μL of 0.2% TFA and desalted on a C18 trap (75 μm × 3 cm, 5−10 μm, 120 Å, YMC gel) at 8 μL/min for 15 min with buffer A (0.1% formic acid) using an Eksigent nano-2D LC system. After desalting, peptides were separated on a C18 column (75 μm × 10 cm, 5 μm, 120 Å, YMC ODS-AQ, Waters, Milford, MA) with an 8 μm emitter tip (New Objective, Woburn, MA) using a 5−40% B (90% acetonitrile in 0.1% formic acid) gradient over 60 min at 300 nL/min. Eluting peptides were sprayed directly into a QSTAR/Pulsar mass spectrometer (Applied Biosystems) and sequenced by tandem mass spectrometry. Survey scans were acquired from m/z 350−1300 with upto three precursors selected for MS/MS using a dynamic exclusion of 45 s. A rolling collision energy was used to promote fragmentation, and the collision energy range was ~20% higher than that used for unlabeled peptides due to iTRAQ tags.

Data Analysis. The MS/MS spectra were extracted and searched against the SwissProt database (version 54.6), human species using ProteinPilot software (v2.0.1, Applied Biosystems)

with the Paragon search algorithm and with the following parameters: trypsin as enzyme (one missed cleavage allowed) and variable modifications for methionine oxidation of cysteine, phosphorylation of serine/threonine/tyrosine, and 8-plex-iTRAQ labeling of N-termini, lysine, and tyrosine. The raw peptide identifications from the Paragon Algorithm (Applied Biosystems) searches were further processed by the Pro Group Algorithm (Applied Biosystems) within the ProteinPilot software set to identify peptides with a confidence threshold 95% (unused confidence threshold Protscore >1.3). Identified phosphopeptides were verified by manual inspection. ProteinPilot was also used to calculate the protein and peptide ratios. For protein ratios, the contribution of each peptide ratio to the overall protein ratio is proportional to the confidence of individual peptide ratio.

RESULTS

Expression and Purification of EGFR. The gene encoding the full-length human EGF receptor (EGFR) was stably transfected into Lec1 CHO cells, which lack the *N*-acetylglucosaminyltransferase I activity essential for synthesis of complex N-linked glycans (*29*). Following methotrexate amplification and selection for high levels of EGFR expression by fluorescence-activated cell sorting, transfected cells were estimated to express at least $\sim 5 \times 10^5$ receptors per cell based on Western blots calibrated with known amounts of standard protein. Initial preparations of EGFR from these cells invariably included a proteolytic fragment of EGFR missing ~20 kD from the C-terminus (*30*, *31*). Efforts to prevent proteolysis reduced but did not eliminate this fragment. A region encoding a hexa-histidine tag followed by a stop codon was thus introduced into the EGFR gene following the position encoding Gly 998, which immediately follows the kinase region (*32*), and this truncated form of EGFR (tEGFR) was expressed in Lec1 cells.

Western blots carried out in reducing and nonreducing conditions showed that tEGFR formed disulfide-linked oligomers. All 50 conserved cysteines in the EGFR extracellular region are involved in disulfide bonds, implicating intracellular cysteines in mediating this oligomerization. To avoid the formation of disulfide-linked tEGFR oligomers without using reducing agents and potentially destabilizing the disulfide-rich extracellular region, surface-exposed intracellular cysteines (Cys 751, Cys 757, and Cys 773) were substituted with serine by site-directed mutagenesis (*32*). A truncated EGFR bearing these cysteine substitutions was expressed in Lec1 cells and proved to be both relatively stable to proteolysis and monomeric in the absence of reducing agents as judged by size-exclusion chromatography. Addition of 0.5 mM dithiothreitol also disrupted unwanted disulfide-mediated oligomers without effect on the ability of tEGFR to bind either EGF or the Fab fragment of the anti-EGFR antibody cetuximab.

Attempts to scale up production of tEGFR to levels needed for structural and biochemical studies were hindered by difficulties growing transfected Lec1 cells above cell densities of $\sim 5 \times 10^5$ cells/mL. HEK GnTi$^-$ cells, which reliably grow to 3−4 million cells/mL and also lack *N*-acetylglucosaminyltransferase I activity (*25*), were thus transfected with a gene encoding tEGFR and a C-terminal hexa-histidine tag inserted into the pLEXm expression vector (*24*). tEGFR expression levels in both transient and stably transfected HEK293 GnTi$^-$ cells were estimated to be at least 5×10^5 receptors per cell on the basis of purification yields from known numbers of cells. tEGFR expression in stably

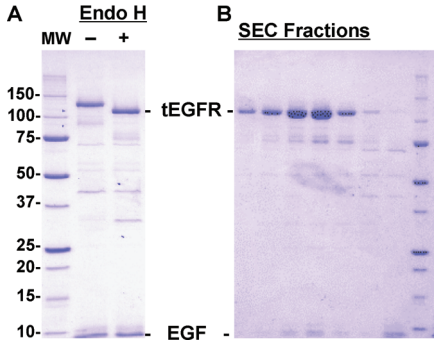

FIGURE 1: tEGFR purification. (A) Coomassie Blue-stained SDS−PAGE analysis of the affinity-purified tEGFR:EGF complex before and after treatment with endoglycosidase H. (B) Coomassie Blue-stained Superose-6 size-exclusion column fractions of the endoglycosidase H-treated tEGFR:EGF complex. The peak elution volume is consistent with a 2:2 EGF:tEGFR complex.

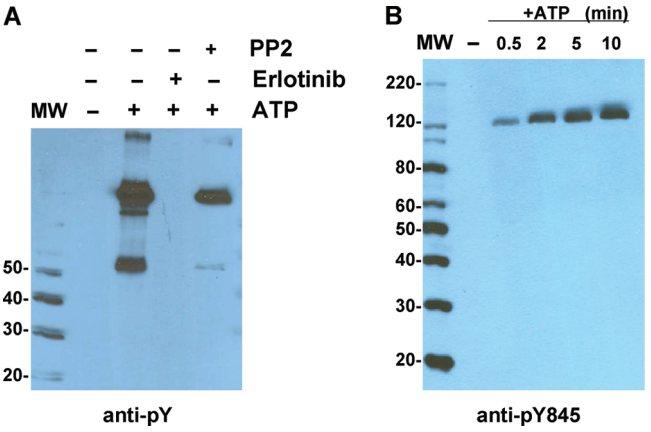

FIGURE 2: tEGFR autophosphorylation. (A) Western blot analysis of the tEGFR:EGF complex before and after the addition of ATP and in the presence and absence of the EGFR inhibitor erlotinib and the Src inhibitor PP2. The antiphosphotyrosine antibody 4G10 was used for detection. The band near 50 kD is likely a C-terminal degradation product following cleavage in the extracellular region. (B) Western blot analysis of the tEGFR:EGF complex at various times (in minutes) following the addition of ATP. A polyclonal antibody specific for EGFR Y845 (Life Sciences) was used.

transfected cells decreased with time, but transient transfection using polyethylenimine (PEI) and square shaker bottles resulted in consistent yields of ~0.2 mg of purified tEGFR per liter of cells and was subsequently pursued (*24*, *26*).

Ni-NTA resin failed to adsorb the bulk of tEGFR from large-scale cell lysates despite the C-terminal hexa-histidine tag. The anti-EGFR monoclonal antibody 528 (MAb528) was thus coupled to a matrix to create an affinity column, which efficiently adsorbed tEGFR from cell lysates (*28*). EGF and the anti-EGFR monoclonal antibody cetuximab both compete with MAb528 for EGFR binding, and both elute tEGFR from the MAb528 column. A combination of endoglycosidases H and F removed N-linked glycosylation (Figure 1A), and size-exclusion chromatography showed the EGF/tEGFR complex to elute at a volume consistent with a 2:2 heterotetramer (Figures 1B and S1 (Supporting Information)). The tEGFR/cetuximab Fab eluted at a volume consistent with a 1:1 complex.

Autophosphorylation of Tyrosine 845. Western blot analysis of purified EGF/tEGFR complex using a phosphotyrosine-specific antibody (4G10) showed it to autophosphorylate following the addition of ATP (Figure 2A). This autophosphorylation

is inhibited by erlotinib, an ErbB inhibitor, but not PP2, an Src inhibitor (Figure 2A). tEGFR contains one of six phosphorylation sites (Y992) previously identified in the C-terminal tail of EGFR (*7*, *33*). tEGFR also includes tyrosine 845 (Y845), which is situated in the activation loop and is known to become phosphorylated in an EGF-dependent manner following EGFR activation and to be phosphorylated by Src (*34*, *35*). A pY845-specific antibody (Life Sciences) recognized tEGFR after incubation with ATP (Figure 2B), and tandem mass spectrometry of trypsinized tEGFR peptides following iTRAQ labeling demonstrates an ~17-fold increase in the amount of a pY845-containing EGFR peptide following the addition of ATP to tEGFR (Table 1 and Figures S2−S6 (Supporting Information)) (*36*). Autophosphorylation of tEGFR at Y845 was inhibited by erlotinib but not PP2, and the levels of threonine phosphorylation detected by mass spectrometry did not change significantly, indicating that the changes in phosphotyrosine levels are not due to variability in protein amounts between samples (Table 1). PP2 appeared to inhibit EGFR activity to a greater extent in the Western blot vs mass spectrometric analysis, although the trends and direction were the same. A possible explanation for this difference is that the kinase reaction was carried out for a shorter time and at a lower temperature for the Western blot analysis.

Table 1: Phosphopeptide Ratios

confidence	sequence	phosphate modification site	+ATP: −ATP	+ATP +Erlotinib: −ATP	+ATP +PP2: −ATP
99	ELVEPL**T**PSGE-APNQALLR	T669	1.14	1.01	1.52
99	LLGAEEKE**Y**H-AEGGK	Y845	16.98	1.71	14.62
99	LLGAEEKE**Y**H-AEGGKVPIK	Y845	5.18	1.27	3.99

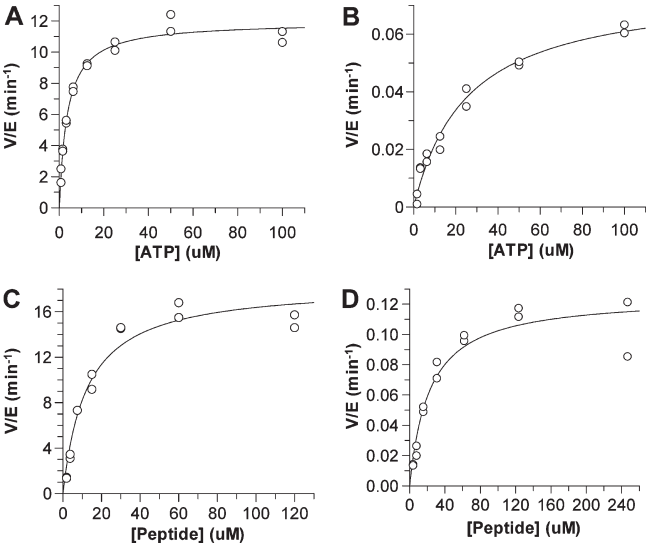

FIGURE 3: Steady-state kinetic analysis of tEGFR. (A) V/E vs [ATP] for EGF/tEGFR with 2 mM Mn^{2+}, 31 μM peptide substrate, and 25 nM enzyme (0.78, 1.56, 3.13, 6.25, 12.5, 25, 50, and 100 μM ATP). (B) V/E vs [ATP] for cetuximab Fab/tEGFR with 2 mM Mn^{2+}, 62 μM peptide substrate, and 125 nM enzyme (1.56, 3.13, 6.25, 12.5, 25, 50, and 100 μM ATP). (C) V/E vs [peptide] for EGF/tEGFR with 2 mM Mn^{2+}, 100 μM ATP, and 25 nM enzyme (1.88, 3.75, 7.5, 15, 30, 60, and 120 μM peptide substrate). (D) V/E vs [peptide] for cetuximab Fab/tEGFR with 2 mM Mn^{2+}, 100 μM ATP, and 125 nM enzyme (6.25, 12.5, 25, 50, 100, 200, 400, and 800 μM peptide substrate).

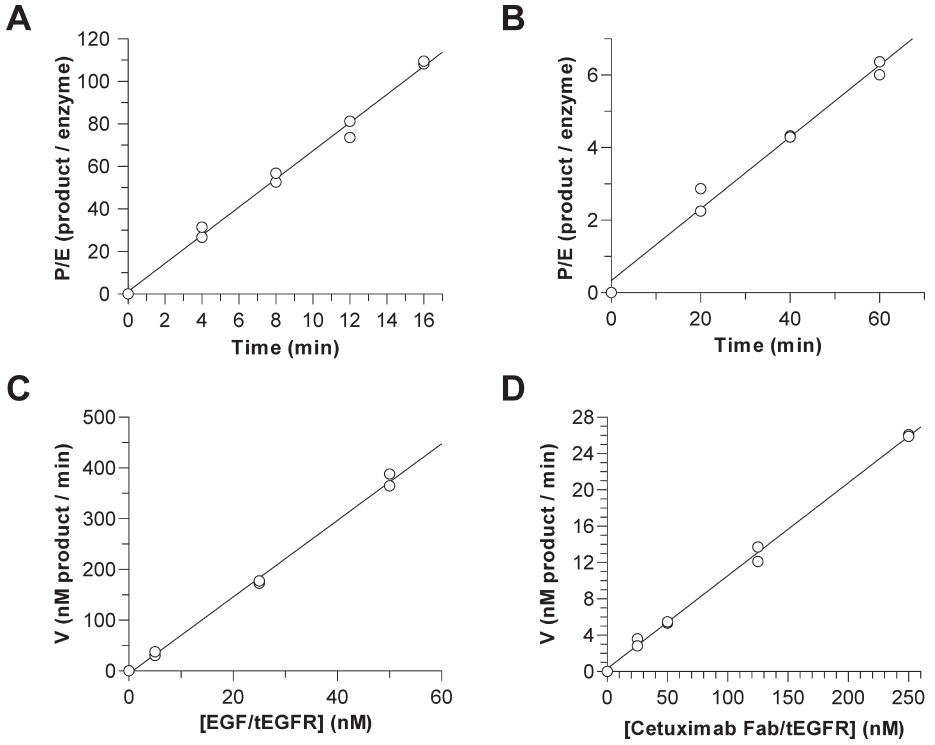

FIGURE 4: tEGFR kinase activity is linear vs time and enzyme concentration. Representative plots illustrating the linearity of enzyme activity with both time and enzyme concentration. Assays for the linear range were performed with 80 μM peptide substrate and 100 μM ATP. (A) P/E vs time for EGF/tEGFR with 2 mM Mn^{2+} and 25 nM enzyme (4, 8, 12, and 16 min time points). (B) P/E vs time for cetuximab Fab/tEGFR with 2 mM Mn^{2+} and 25 nM enzyme (20, 40, 60 min time points). (C) Activity vs enzyme concentration for EGF/tEGFR with 2 mM Mn^{2+} (5, 25, and 50 nM enzyme). (D) Activity vs enzyme concentration for cetuximab Fab/tEGFR with 2 mM Mn^{2+} (25, 50, 125, and 250 nM enzyme).

Table 2: Comparison of Specific Activities

ligand	divalent cation	V/E (min^{-1})[a]
cetux Fab	10 mM Mg^{2+}	0.03 min^{-1}
cetux Fab	2 mM Mn^{2+}	0.10 min^{-1}
EGF	10 mM Mg^{2+}	16 min^{-1}
EGF	2 mM Mn^{2+}	15 min^{-1}

[a]Specific activities were measured with 62 μM peptide substrate and 100 μM ATP.

Table 3: Enzymatic Parameters

ligand	divalent cation	K_m^{app} peptide (μM)	K_m^{app} ATP (μM)	k_{cat} (min^{-1})
EGF	10 mM Mg^{2+}	41 ± 8^a	47 ± 12^b	24 ± 2^a
EGF	2 mM Mn^{2+}	12 ± 2^a	3.6 ± 0.3^c	18 ± 1^a
cetux Fab	2 mM Mn^{2+}	23 ± 5^a	25 ± 4^d	0.13 ± 0.01^a

[a]K_m^{app} peptide and k_{cat} values were obtained with 100 μM ATP. [b]K_m^{app} ATP value was obtained with 124 μM peptide substrate. [c]K_m^{app} ATP value was obtained with 31 μM peptide substrate. [d]K_m^{app} ATP value was obtained with 62 μM peptide substrate.

Characterization of the Kinase Activity of tEGFR. For a quantitative analysis of the kinase activity of tEGFR, we used a radiometric assay to compare the effects of EGF and the Fab fragment cetuximab, an anti-EGFR antibody that blocks EGF binding and formation of extracellular EGFR dimers, on the ability of tEGFR to phosphorylate a biotinylated peptide substrate (Figure 3). Steady-state kinase assays were carried out using a consensus peptide substrate with sequence RAHEEIY-HFFFAKKK and repeated using either Mg^{2+} or Mn^{2+} as the divalent metal ion. Under the conditions of our assay, the activities of EGF/tEGFR and cetuximab/tEGFR were shown to be linear vs time and enzyme concentration, indicating that neither tEGFR oligomerization nor degradation was likely to be influencing activity in the ranges investigated (Figure 4). For EGF/tEGFR, the K_m^{app} for ATP was nearly 13-fold lower with Mn^{2+} (3.6 μM) than with Mg^{2+} (47 μM). Lower K_m values for ATP in the presence of Mn^{2+} vs Mg^{2+} are commonly observed with protein kinases, presumably owing to the increased nucleotide affinity of Mn^{2+} (*37*, *38*). Mg^{2+} vs Mn^{2+} had a smaller effect on the apparent k_{cat} (24 vs 18 min^{-1}, respectively) and K_m for peptide substrate (41 vs 12 μM) values, which were within 5-fold of one another.

The low activity of cetuximab/tEGFR precluded measurement of a full range of catalytic parameters with the Mg^{2+} ion, but at fixed substrate concentration, the observed kinase activity was ~500-fold lower than that of EGF/tEGFR in the presence of Mg^{2+} and ~150-fold lower in the presence of Mn^{2+} (Table 2). This observation was in the range of the k_{cat}/K_m effects for ATP (920-fold) and peptide (260-fold). The major effect of ligand binding was on apparent k_{cat} values, which were ~140-fold, but 2-fold (peptide) and 7-fold (ATP) increases in apparent K_m values were observed in the presence of cetuximab (Table 3). Interestingly, addition of excess EGF to cetuximab/tEGFR did not significantly stimulate kinase activity, suggesting that exchange of these protein ligands is slow on the time scale of these assays.

We then evaluated the effects of EGFR kinase inhibitors erlotinib and lapatinib on the kinase activity of EGF and cetuximab complexed forms of tEGFR (Figure 5). Erlotinib showed a 10-fold enhanced potency against EGF/tEGFR compared to that of cetuximab/tEGFR (Table 4). Conversely, lapatinib inhibited cetuximab/tEGFR relative to EGF/tEGFR by a 4-fold margin. Taken together, these data are consistent with the prevailing view that erlotinib targets the active EGFR kinase conformation, whereas lapatinib preferentially binds to the inactive conformation (*32*, *39*).

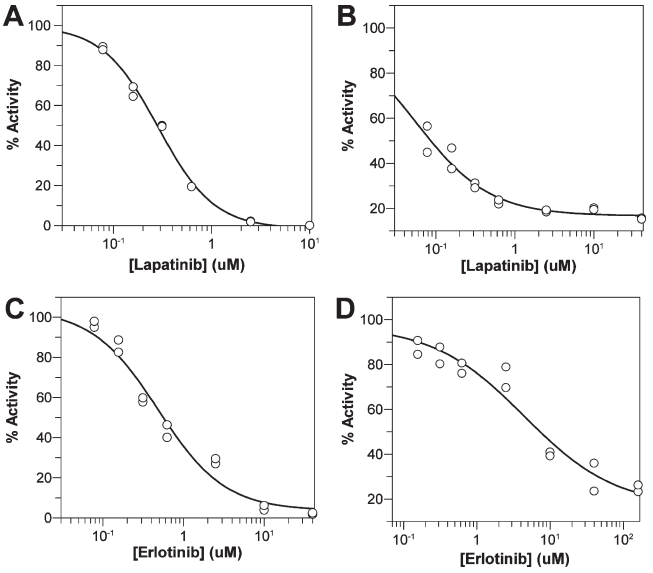

FIGURE 5: tEGFR kinase inhibition by lapatinib and erlotinib. Inhibition assays were run with 10 μM ATP, 30 μM peptide, 2 mM Mn^{2+}, 25 nM enzyme, and 0.15% DMSO. (A) Inhibition of EGF/tEGFR by lapatinib. Lapatinib was preincubated with enzyme on ice for 10 min, and the reaction proceeded for 6 min. (B) Inhibition of cetuximab. Fab/tEGFR was preincubated with enzyme on ice, and the reaction proceeded for 40 min. (C) Inhibition of EGF/tEGFR by erlotinib. Erlotinib was preincubated with enzyme at 30 °C for 10 min, and the reaction proceeded for 5 min. (D) Inhibition of cetuximab Fab/tEGFR by erlotinib. Erlotinib was preincubated with enzyme at 30 °C for 10 min, and the reaction proceeded for 40 min.

Table 4: Inhibitor Effects

inhibitor	ligand	IC_{50} (μM)[a]
lapatinib	EGF	0.281 ± 0.015
lapatinib	cetux Fab	0.056 ± 0.010
erlotinib	EGF	0.486 ± 0.089
erlotinib	cetux Fab	4.4 ± 2.1

[a]IC_{50} values were obtained with 2 mM Mn^{2+}, 30 μM peptide substrate, and 10 μM ATP.

DISCUSSION

We have developed a strategy to produce a form of the EGF receptor that is activated by ligand binding and suitable for structural, biophysical, and biochemical studies. Steps have been taken to maximize yields and minimize both the time and cost of production as well as heterogeneity arising from glycosylation and proteolysis. In particular, large-scale transient transfection of the EGFR gene into HEK293 GnTi$^-$ cells using PEI as a transfection reagent proved a cost- and time-effective approach that yields ~0.2 mg of purified EGFR per liter of transfected cells and enables efficient removal of N-linked glycosylation using endoglycosidases H and F. Eliminating the structural and chemical heterogeneity of attached carbohydrates often proves beneficial to the growth of diffraction-quality crystals (*40*).

Heterogeneity in purified EGFR also arose from proteolysis of the C-terminal tail, which proved difficult to avoid completely, and a premature stop codon that eliminated the C-terminal tail was thus introduced immediately following the region encoding the EGFR kinase domain. Coupled with efficient deglycosylation of HEK293 GnTi$^-$ cell-expressed EGFR, truncation of EGFR following the kinase domain allowed purification of a relatively homogeneous form EGFR that is activated by ligand binding. As also observed by Springer and colleagues (*21*), tEGFR is solubilized well in both Triton X-100 and dodecylmaltoside, is monomeric in the absence of ligand, and is dimeric in the presence of EGF as judged by size-exclusion chromatography.

Additional heterogeneity arose from the formation of unwanted disulfide-linked EGFR oligomers in mildly oxidizing initial purification conditions, presumably mediated by cytoplasmic cysteines that are reduced in normal cell environments. Two approaches, mutagenesis of exposed cytoplasmic cysteines and addition of a small amount of reducing agent, both successfully eliminated unwanted EGFR oligomers. Concerns that a small amount of reducing agent might disrupt the structure and function of the heavily disulfide-linked extracellular region were overcome when the inclusion of 0.5 mM dithiothreitol failed to diminish ligand binding activity or lead to oligomerization through transient reduction of extracellular disulfide bonds. To avoid complications owing to possible effects of cysteine mutations on EGFR enzymatic activity, 0.5 mM dithiothreitol was used during purification to produce native tEGFR for the studies reported here.

Preparation of purified tEGFR allowed quantitative characterization of its kinase activity. Early published reports identified six autophosphorylation sites in the EGFR C-terminal tail but no sites in the kinase region itself (*7*, *33*). Later studies showed that a tyrosine on the kinase activation loop, Y845, is phosphorylated by the Src kinase and that phosphorylation of Y845 influences EGFR function (*34*, *35*). Phosphoryation of Y845 is not required for EGFR activity, however (*41*). More recently, Arteaga and colleagues showed that Y845 becomes phosphorylated following TGFα stimulation or introduction of oncogenic EGFR mutations and that this Y845 phosphorylation is dependent on EGFR kinase activity (*42*). Using purified tEGFR and tandem mass spectrometry, we now demonstrate that EGFR itself is capable of phosphorylating Y845. It is well established that phosphorylation of activation loop tyrosines increases the activity of several kinases (*43*), and phosphorylation of Y845 seems likely to promote or stabilize EGFR activity and modulate EGFR signaling.

Comparison of the kinase activities of EGF/tEGFR and cetuximab/tEGFR demonstrates that the ligand stimulates an ~500-fold increase in catalytic activity (k_{cat}) and that the effect of ligand binding to tEGFR is predominantly on k_{cat} rather than substrate K_m values. This observation suggests that substrate binding is likely to be only modestly perturbed in the cetuximab/tEGFR complex. Structural studies on the Abl tyrosine kinase support the idea that interactions with the peptide substrate can be maintained despite kinase activation loop and C-lobe conformations that appear inconsistent with catalysis (*44*). In this case, the orientation of the two substrates and/or placement of key catalytic residues appear distorted from active conformations. A similar mechanism may underlie our observations with EGFR.

Prior quantitative studies of EGFR/ErbB enzymatic activity have primarily utilized soluble intracellular domain fragments or incompletely characterized EGFR (*11*, *17*−*20*). In particular, one recent approach mimicked the high local concentrations achieved in a membrane environment by tethering the EGFR kinase domain to lipid vesicles via a hexa-histidine tag (*11*). Stimulation of kinase activity by up to 20-fold was observed following vesicle targeting, consistent with a key role for kinase dimerization in activation.

To our knowledge, our study describes the first detailed kinetic analysis of near full-length EGFR in purified form. By comparing EGF and cetuximab-complexed forms of tEGFR, we have shown a 500-fold activation between autoinhibited and stimulated forms. Elimination of the C-terminal tail may have influenced our results, but this change in activity is some 25-fold greater than the stimulation observed with vesicle activation. This 500-fold differential is also considerably larger than measurements of kinase domains bearing activating mutations (*11*, *45*, *46*). Taken together, these results suggest that the kinase domain-only assays incompletely recapitulate full activation/inhibition of the EGFR kinase. The differences observed between isolated kinase regions and a more intact form of the receptor are perhaps not surprising as the ligand-bound extracellular regions and the juxtamembrane regions must contribute to stronger dimerization if not also stereochemically favorable apposition of the kinase domains (*47*, *48*).

Of potential clinical interest among the results reported here is the relative inhibitory potencies of the two anticancer agents erlotinib and lapatinib, which structural studies have shown bind to active and inactive EGFR kinase conformations, respectively (*11*, *32*, *39*). We observed the expected trend that erlotinib is more effective at inhibiting the ligand-activated EGFR kinase and that lapatinib is more effective at inhibiting inactive EGFR. This observation suggests the potential for therapeutic synergy between cetuximab and lapatinib. The relative selectivity of erlotinib and lapatinib for their preferred enzyme forms was only 5−10-fold, however, which was less than expected on the basis of the much larger relative difference in kinase activity in the presence and absence of ligand. Either substantial crossover binding of these inhibitors for alternate EGFR kinase conformations occurs or an unexpectedly high interconversion between active and inactive kinase conformations may occur irrespective of receptor dimerzation. Given the conditions of our assay and the 7-fold higher K_m for ATP of cetuximab complexed with tEGFR compared with that of EGF/tEGFR, the K_i values deduced for lapatinib blocking the inhibited and active enzyme forms are essentially identical. These findings run contrary to the concept of truly conformation-specific EGFR kinase inhibitors and suggest that further investigation of inhibitor-bound conformations of the EGFR kinase may prove illuminating.

A final observation to emerge from our results is that even the inactive EGFR conformation observed crystallographically appears capable of catalyzing phosphoryl transfer, albeit at a significantly reduced rate. The differences in substrate K_m values observed for the cetuximab vs EGF bound forms of tEGFR suggest that the residual kinase activity in the antibody-complexed EGFR arises from a different kinase conformation. Had the lower activity of the cetuximab/tEGFR complex resulted solely from shifting the conformational equilibrium of the kinase region away from the active conformation, one would expect to observe lower k_{cat} values but unaffected K_m values. Although 500-fold lower than the EGF-tEGFR rate, the catalytic power of cetuximab/tEGFR is still more than 10,000-fold greater than the uncatalyzed phosphoryl transfer reaction (*49*), indicating that substantial transition state stabilization still occurs in this state.

ACKNOWLEDGMENT

We thank members of the Cole and Leahy laboratories for helpful suggestions and discussions and M. Lemmon, C. Mukherjee, C. Hann, W. Bornmann, and D. Meyers for assistance and/or reagents.

SUPPORTING INFORMATION AVAILABLE

Size-exclusion chromatography and quantification of phosphotyrosine 845 and 974, phosphothreonine 669, and phosphoserine 967. This material is available free of charge via the Internet at http://pubs.acs.org.

REFERENCES

1. Blume-Jensen, P., and Hunter, T. (2001) Oncogenic kinase signalling. *Nature 411*, 355–365.
2. Ushiro, H., and Cohen, S. (1980) Identification of phosphotyrosine as a product of epidermal growth factor-activated protein kinase in A-431 cell membranes. *J. Biol. Chem. 255*, 8363–8365.
3. Schlessinger, J. (2000) Cell signaling by receptor tyrosine kinases. *Cell 103*, 211–225.
4. Yarden, Y., and Schlessinger, J. (1987) Epidermal growth factor induces rapid, reversible aggregation of the purified epidermal growth factor receptor. *Biochemistry 26*, 1443–1451.
5. Heldin, C. H. (1995) Dimerization of cell surface receptors in signal transduction. *Cell 80*, 213–223.
6. Holbro, T., and Hynes, N. E. (2004) ErbB receptors: directing key signaling networks throughout life. *Annu. Rev. Pharmacol. Toxicol. 44*, 195–217.
7. Olayioye, M. A., Neve, R. M., Lane, H. A., and Hynes, N. E. (2000) The ErbB signaling network: receptor heterodimerization in development and cancer. *EMBO J. 19*, 3159–3167.
8. Hynes, N. E., and Lane, H. A. (2005) ERBB receptors and cancer: the complexity of targeted inhibitors. *Nat. Rev. Cancer 5*, 341–354.
9. Johnston, J. B., Navaratnam, S., Pitz, M. W., Maniate, J. M., Wiechec, E., Baust, H., Gingerich, J., Skliris, G. P., Murphy, L. C., and Los, M. (2006) Targeting the EGFR pathway for cancer therapy. *Curr. Med. Chem. 13*, 3483–3492.
10. Burgess, A. W., Cho, H. S., Eigenbrot, C., Ferguson, K. M., Garrett, T. P., Leahy, D. J., Lemmon, M. A., Sliwkowski, M. X., Ward, C. W., and Yokoyama, S. (2003) An open-and-shut case? Recent insights into the activation of EGF/ErbB receptors. *Mol. Cell 12*, 541–552.
11. Zhang, X., Gureasko, J., Shen, K., Cole, P. A., and Kuriyan, J. (2006) An allosteric mechanism for activation of the kinase domain of epidermal growth factor receptor. *Cell 125*, 1137–1149.
12. Bouyain, S., Longo, P. A., Li, S., Ferguson, K. M., and Leahy, D. J. (2005) The extracellular region of ErbB4 adopts a tethered conformation in the absence of ligand. *Proc. Natl. Acad. Sci. U.S.A. 102*, 15024–15029.
13. Cho, H. S., and Leahy, D. J. (2002) Structure of the extracellular region of HER3 reveals an interdomain tether. *Science 297*, 1330–1333.
14. Ferguson, K. M., Berger, M. B., Mendrola, J. M., Cho, H. S., Leahy, D. J., and Lemmon, M. A. (2003) EGF activates its receptor by removing interactions that autoinhibit ectodomain dimerization. *Mol. Cell 11*, 507–517.
15. Garrett, T. P., McKern, N. M., Lou, M., Elleman, T. C., Adams, T. E., Lovrecz, G. O., Zhu, H. J., Walker, F., Frenkel, M. J., Hoyne, P. A., Jorissen, R. N., Nice, E. C., Burgess, A. W., and Ward, C. W. (2002) Crystal structure of a truncated epidermal growth factor receptor extracellular domain bound to transforming growth factor alpha. *Cell 110*, 763–773.
16. Ogiso, H., Ishitani, R., Nureki, O., Fukai, S., Yamanaka, M., Kim, J. H., Saito, K., Sakamoto, A., Inoue, M., Shirouzu, M., and Yokoyama, S. (2002) Crystal structure of the complex of human epidermal growth factor and receptor extracellular domains. *Cell 110*, 775–787.
17. Brignola, P. S., Lackey, K., Kadwell, S. H., Hoffman, C., Horne, E., Carter, H. L., Stuart, J. D., Blackburn, K., Moyer, M. B., Alligood, K. J., Knight, W. B., and Wood, E. R. (2002) Comparison of the biochemical and kinetic properties of the type 1 receptor tyrosine kinase intracellular domains. Demonstration of differential sensitivity to kinase inhibitors. *J. Biol. Chem. 277*, 1576–1585.
18. Honegger, A., Dull, T. J., Szapary, D., Komoriya, A., Kris, R., Ullrich, A., and Schlessinger, J. (1988) Kinetic parameters of the protein tyrosine kinase activity of EGF-receptor mutants with individually altered autophosphorylation sites. *EMBO J. 7*, 3053–3060.
19. Jan, A. Y., Johnson, E. F., Diamonti, A. J., Carraway, I. K., and Anderson, K. S. (2000) Insights into the HER-2 receptor tyrosine kinase mechanism and substrate specificity using a transient kinetic analysis. *Biochemistry 39*, 9786–9803.
20. Qiu, C., Tarrant, M. K., Choi, S. H., Sathyamurthy, A., Bose, R., Banjade, S., Pal, A., Bornmann, W. G., Lemmon, M. A., Cole, P. A., and Leahy, D. J. (2008) Mechanism of activation and inhibition of the HER4/ErbB4 kinase. *Structure 16*, 460–467.
21. Mi, L. Z., Grey, M. J., Nishida, N., Walz, T., Lu, C., and Springer, T. A. (2008) Functional and structural stability of the epidermal growth factor receptor in detergent micelles and phospholipid nanodiscs. *Biochemistry 47*, 10314–10323.
22. Petrov, K. G., Zhang, Y. M., Carter, M., Cockerill, G. S., Dickerson, S., Gauthier, C. A., Guo, Y., Mook, R. A., Jr., Rusnak, D. W., Walker, A. L., Wood, E. R., and Lackey, K. E. (2006) Optimization and SAR for dual ErbB-1/ErbB-2 tyrosine kinase inhibition in the 6-furanylquinazoline series. *Bioorg. Med. Chem. Lett. 16*, 4686–4691.
23. Nabavi, S., and Nazar, R. N. (2005) Simplified one-tube "megaprimer" polymerase chain reaction mutagenesis. *Anal. Biochem. 345*, 346–348.
24. Aricescu, A. R., Lu, W., and Jones, E. Y. (2006) A time- and cost-efficient system for high-level protein production in mammalian cells. *Acta Crystallogr., Sect. D 62*, 1243–1250.
25. Reeves, P. J., Kim, J. M., and Khorana, H. G. (2002) Structure and function in rhodopsin: a tetracycline-inducible system in stable mammalian cell lines for high-level expression of opsin mutants. *Proc. Natl. Acad. Sci. U.S.A. 99*, 13413–13418.
26. Muller, N., Girard, P., Hacker, D. L., Jordan, M., and Wurm, F. M. (2005) Orbital shaker technology for the cultivation of mammalian cells in suspension. *Biotechnol. Bioeng. 89*, 400–406.
27. Geisbrecht, B. V., Bouyain, S., and Pop, M. (2006) An optimized system for expression and purification of secreted bacterial proteins. *Protein Expression Purif. 46*, 23–32.
28. Sato, J. D., Kawamoto, T., Le, A. D., Mendelsohn, J., Polikoff, J., and Sato, G. H. (1983) Biological effects in vitro of monoclonal antibodies to human epidermal growth factor receptors. *Mol. Biol. Med. 1*, 511–529.
29. Stanley, P. (1989) Chinese hamster ovary cell mutants with multiple glycosylation defects for production of glycoproteins with minimal carbohydrate heterogeneity. *Mol. Cell. Biol. 9*, 377–383.
30. Cohen, S., Carpenter, G., and King, L., Jr. (1980) Epidermal growth factor-receptor-protein kinase interactions. Co-purification of receptor and epidermal growth factor-enhanced phosphorylation activity. *J. Biol. Chem. 255*, 4834–4842.
31. Cohen, S., Ushiro, H., Stoscheck, C., and Chinkers, M. (1982) A native 170,000 epidermal growth factor receptor-kinase complex from shed plasma membrane vesicles. *J. Biol. Chem. 257*, 1523–1531.
32. Stamos, J., Sliwkowski, M. X., and Eigenbrot, C. (2002) Structure of the epidermal growth factor receptor kinase domain alone and in complex with a 4-anilinoquinazoline inhibitor. *J. Biol. Chem. 277*, 46265–46272.
33. Margolis, B. L., Lax, I., Kris, R., Dombalagian, M., Honegger, A. M., Howk, R., Givol, D., Ullrich, A., and Schlessinger, J. (1989) All autophosphorylation sites of epidermal growth factor (EGF) receptor and HER2/neu are located in their carboxyl-terminal tails. Identification of a novel site in EGF receptor. *J. Biol. Chem. 264*, 10667–10671.
34. Biscardi, J. S., Maa, M. C., Tice, D. A., Cox, M. E., Leu, T. H., and Parsons, S. J. (1999) c-Src-mediated phosphorylation of the epidermal growth factor receptor on Tyr845 and Tyr1101 is associated with modulation of receptor function. *J. Biol. Chem. 274*, 8335–8343.
35. Sato, K., Sato, A., Aoto, M., and Fukami, Y. (1995) c-Src phosphorylates epidermal growth factor receptor on tyrosine 845. *Biochem. Biophys. Res. Commun. 215*, 1078–1087.
36. Zieske, L. R. (2006) A perspective on the use of iTRAQ reagent technology for protein complex and profiling studies. *J. Exp. Bot. 57*, 1501–1508.
37. Adams, J. A., and Taylor, S. S. (1993) Divalent metal ions influence catalysis and active-site accessibility in the cAMP-dependent protein kinase. *Protein Sci. 2*, 2177–2186.
38. Grace, M. R., Walsh, C. T., and Cole, P. A. (1997) Divalent ion effects and insights into the catalytic mechanism of protein tyrosine kinase Csk. *Biochemistry 36*, 1874–1881.
39. Wood, E. R., Truesdale, A. T., McDonald, O. B., Yuan, D., Hassell, A., Dickerson, S. H., Ellis, B., Pennisi, C., Horne, E., Lackey, K., Alligood, K. J., Rusnak, D. W., Gilmer, T. M., and Shewchuk, L. (2004) A unique structure for epidermal growth factor receptor bound to GW572016 (Lapatinib): relationships among protein conforma-

tion, inhibitor off-rate, and receptor activity in tumor cells. *Cancer Res. 64*, 6652–6659.
40. Grueninger-Leitch, F., D'Arcy, A., D'Arcy, B., and Chene, C. (1996) Deglycosylation of proteins for crystallization using recombinant fusion protein glycosidases. *Protein Sci. 5*, 2617–2622.
41. Gotoh, N., Tojo, A., Hino, M., Yazaki, Y., and Shibuya, M. (1992) A highly conserved tyrosine residue at codon 845 within the kinase domain is not required for the transforming activity of human epidermal growth factor receptor. *Biochem. Biophys. Res. Commun. 186*, 768–774.
42. Yang, S., Park, K., Turkson, J., and Arteaga, C. L. (2008) Ligand-independent phosphorylation of Y869 (Y845) links mutant EGFR signaling to stat-mediated gene expression. *Exp. Cell Res. 314*, 413–419.
43. Huse, M., and Kuriyan, J. (2002) The conformational plasticity of protein kinases. *Cell 109*, 275–282.
44. Levinson, N. M., Kuchment, O., Shen, K., Young, M. A., Koldobskiy, M., Karplus, M., Cole, P. A., and Kuriyan, J. (2006) A Src-like inactive conformation in the abl tyrosine kinase domain. *PLoS Biol. 4*, e144.
45. Yun, C. H., Mengwasser, K. E., Toms, A. V., Woo, M. S., Greulich, H., Wong, K. K., Meyerson, M., and Eck, M. J. (2008) The T790M mutation in EGFR kinase causes drug resistance by increasing the affinity for ATP. *Proc. Natl. Acad. Sci. U.S.A. 105*, 2070–2075.
46. Yun, C. H., Boggon, T. J., Li, Y., Woo, M. S., Greulich, H., Meyerson, M., and Eck, M. J. (2007) Structures of lung cancer-derived EGFR mutants and inhibitor complexes: mechanism of activation and insights into differential inhibitor sensitivity. *Cancer Cell 11*, 217–227.
47. Ferguson, K. M., Darling, P. J., Mohan, M. J., Macatee, T. L., and Lemmon, M. A. (2000) Extracellular domains drive homo- but not hetero-dimerization of erbB receptors. *EMBO J. 19*, 4632–4643.
48. Thiel, K. W., and Carpenter, G. (2007) Epidermal growth factor receptor juxtamembrane region regulates allosteric tyrosine kinase activation. *Proc. Natl. Acad. Sci. U.S.A. 104*, 19238–19243.
49. Van Wazer, J. R., Griffith, E. J., and McCullough, J. F. (1955) Structure and properties of the condensed phosphates. VII. Hydrolytic degradation of pyro- and tripolyphosphate. *J. Am. Chem. Soc. 77*, 287–291.